CALIFORNIA PATH PROGRAM
INSTITUTE OF TRANSPORTATION STUDIES
UNIVERSITY OF CALIFORNIA, BERKELEY

Design, Modeling and Control of Steering and Braking for an Urban Electric Vehicle

Dragos Maciuca

California PATH Working Paper
UCB-ITS-PWP-96-11

This work was performed as part of the California PATH Program of the University of California, in cooperation with the State of California Business, Transportation, and Housing Agency, Department of Transportation; and the United States Department Transportation, Federal Highway Administration.

August 1996

ISSN 1055-1417

Design, Modeling and Control of Steering and Braking for an Urban Electric Vehicle

Dragos Maciuca

PATH Report

A Research Exchange Between
Partners for Advanced Transit and Highways (PATH)
University of California at Berkeley

and

Institut National de Recherche en
Informatique et en Automatique (INRIA)
Rocquencourt, France
Programme Praxitèle

Praxitèle

Abstract

Design, Modeling and Control of Steering and Braking for an Urban Electric Vehicle

Dragos B. Maciuca

August 1, 1996

Keywords: Advanced Public Transportation Systems, Automatic Braking, Electric Vehicles, Personal Rapid Transit, Public Transit, Advanced Vehicle Control Systems

This report presents the results of a scientific exchange with Programme Praxitèle of the Institut National de Recherche en Informatique et en Automatique (INRIA) in Rocquencourt, France. The Praxitèle Program provides a combination of public transport and private vehicles. It makes use of innovative techniques to provide people with self-service access to small electric cars. The research involved the design modification, modeling and control of the automatic steering and braking systems of one such urban electric vehicle. The vehicle is equipped with four-wheel independent drive, four-wheel independent braking and four-wheel steering. Control algorithms were developed for steering and braking. Simulation results show the feasibility of these algorithms.

Acknowledgments

This work was performed as part of an scientific exchange between California PATH Program of the University of California and Programme Praxitèle of the Institut National de Recherche en Informatique et en Automatique (INRIA) in Rocquencourt, France. The research was fully funded by INRIA.

Many thanks go to Prof. Michel Parent for allowing this exchange to happen and providing me with an exciting research environment. Thanks also go to Prof. Pravin Varaiya and Prof. Karl Hedrick for facilitating this exchange. Last, but of course not least, thanks to everybody in the lab for being so helpful, understanding and fun.

Executive Summary

This report presents the results of a scientific exchange with Programme Praxitèle of the Institut National de Recherche en Informatique et en Automatique (INRIA) in Rocquencourt, France. The Praxitèle Program provides a combination of public transport and private vehicles. It makes use of innovative techniques to provide people with self-service access to small electric cars. The research involved the design modification, modeling and control of the automatic steering and braking systems of one such urban electric vehicle

The Praxitèle vehicle is a two-passenger electric vehicle. It is capable of speeds up to 25Km/h. The four lead-acid batteries provide it with a range of 200Km. The vehicle has many components that facilitate control. It features four-wheel drive, four-wheel electric independent braking, and four wheel steering. The steering is controlled by a single actuator. Such independent methods of actuation present interesting challenges from a control and stability point of view. The following sections will attempt to give an initial look at the dynamics and control of the steering and braking of this vehicle.

The first challenge was to modify the design of the four-wheel steering mechanism in order to achieve the correct center of curvature. The mechanism, as implemented, generates a large amount of tire slip due to a discrepancy between the front and rear steering angle. It was essential to devise a method that would require the minimum number of modifications to the system. A simple solution was found that requires only the replacement of the front and rear steering crank. Implementation of this method will provide the correct center of curvature and considerably reduce tire slip in turns.

A model of the steering mechanism was also developed. The steering actuator is made up of a linear actuator and two four-bar mechanisms. The model includes the dynamics of the linear actuator and the kinematics of the four-bar mechanism. The model was then used to develop a controller that uses the steering angle as the desired output and the voltage to the actuator as the input. Due to the nonlinearities in the system, a Sliding Mode Controller was suggested. A multiple-surface version of this techniques was used in order to avoid differentiating uncertainties. Simulation results show the feasibility of this controller.

A model and controller of the brake actuation system were also developed. The brake actuator consists of an electric motor and drum brakes. The model includes the dynamics of the motor as

well as the dynamics of the drum brakes. A nonlinear controller was again used to control the brakes. Simulation results show good tracking performance.

This research was beneficial to both PATH and INRIA. PATH's benefit derives from learning the approaches that other researchers have from the same challenges. INRIA's benefit was learning different design, modeling and control techniques applied to their challenges.

1. Introduction

This paper presents the research conducted at INRIA, Rocquencourt, France in the Programme Praxitèle. The research was part of a scientific exchange between PATH and INRIA and was supported in its entirety by INRIA's Programme Praxitèle. The research was an initial study of the dynamics and control for a small urban electric vehicle. Such vehicle will be used as part of the Praxitèle program.

1.1 INRIA

INRIA, Institut National de Recherche en Informatique et en Automatique, is the French National Institute for Research in computer Science and Control. Its scientific policies are defined in response to the needs of the manufacturers and end users of information technology. INRIA contributes in its turn to the advancement of knowledge and to the development of the most highly advanced techniques.

There are six fields of research that bring together researchers in mathematics, control and information technology:

- parallel architectures, databases, networks and distributed systems
- symbolic computing, programming, and software engineering
- artificial intelligence, cognitive systems, and man-machine interaction
- robotics, image and vision
- signal processing, control, and manufacturing automation
- scientific computing, numerical software, and CAE.

The basic concept of a research project is to encourage initiative on the part of the researchers, while providing them with support from the engineers, technicians and administrative staff. This policy demonstrates the advantages of a decentralized organization: greater flexibility, faster reaction time and increased responsibility. There are over 1400 people working at INRIA including some 1000 scientists and 750 temporary outside researchers (including 100 invited foreign researchers). INRIA's 1995 budget was FF 520 million (US$ 100 million).

1.2 Programme Praxitèle

Praxiteles was a fourth century Greek sculptor whose works, including the Labyrinth, captured the essence of life in his time. If he were alive today, he would no doubt agree that life is all about movement, interaction and development. That is why his name was chosen for this new and innovative transport service.

Private cars give their owners freedom and independence. Public transport takes up less space and saves energy. Praxitèle provides a combination of public transport and private vehicles. It makes use of innovative techniques to provide people with self-service access to small electric cars. This concept has been developed by manufacturers from a number of industrial sectors working closely with major research organizations.

Praxitèle lends itself to all forms of local transport. It can be used as
- a supplement to public transport
- a complement to a city center's traffic management
- an on-site transport service in commercial or industrial zones
- public transport during low traffic periods or in sparsely populated areas
- a tourist facility

1.3 The Praxitèle Research Group

The group's strengths are real-time programming and distributed computing. Image processing and sensor development are also emphasized.

Of particular interest are two programs developed by INRIA and available as freeware. The first one, called ORCAD generates real-time C code based on the interaction between control modules. Synchronous, asynchronous and interrup inputs and outputs can be specified. The second one is called SciLab. It is similar with Matlab. Although not as powerful as Matlab, it has a nice animation package.

The program director, Professor Michel Parent, encourages research exchanges such as this one.

1.4 The Praxitèle Vehicle

The Praxitèle vehicle is a two-passenger electric vehicle. It is capable of speeds up to 25Km/h. The four lead-acid batteries provide it with a range of 200Km. The vehicle has many components that facilitate control. It features four-wheel drive, four-wheel electric independent braking, and four wheel steering. The steering is controlled by a single actuator. Such independent methods of actuation present interesting challenges from a control and stability point of view. The following sections will attempt to give an initial look at the dynamics and control of the steering and braking of this vehicle.

2. Steering

2.1 Description

The vehicle features four-wheel steering controlled from a single actuator. The front and rear tires are supposed to have equal and opposite steering angles. A diagram of the current steering system is shown in figure 1. There are however some problems with this design. Ideally the Ackerman steering angle must be adjusted such that the perpendiculars to each tire meet at the center of the turn that the vehicle is performing. As such, in a front steering vehicle, the perpendiculars to the front tires must meet on the extension of the rear axle. For a four wheel steering vehicle, the perpendiculars to all tires should meet on an imaginary line parallel and equidistant from the front and rear axles (lateral centerline). However, as figure 2 shows, the perpendiculars to the front tires meet on the extension of the rear axle and the perpendiculars to the rear tires meet on the extension of the front axle. The major drawback of this situation is a large amount of slip during cornering with large steering angles.

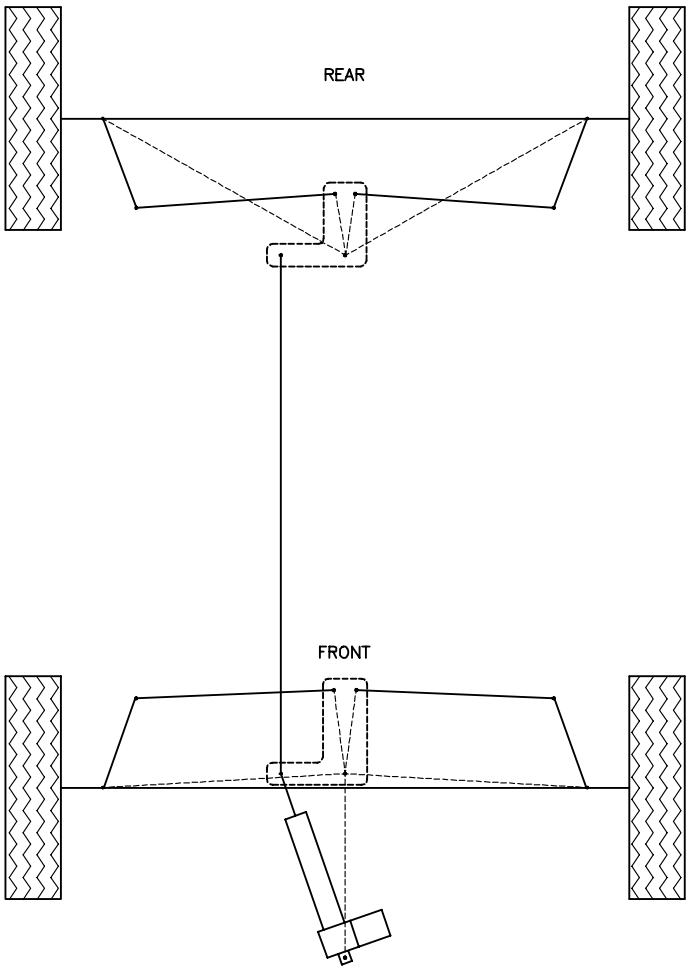

Figure 1. Current Steering Mechanism.

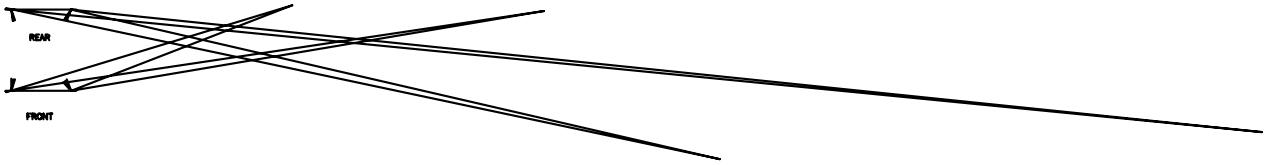

Figure 2. Current Steering Configuration Center of Curvature.

Furthermore, it can be seen from figure 1 that the steering system is not symmetric about the lateral centerline. This situation suggests that the front and rear steering angles will not be equal. This can be easily observed by comparing figures 3 and 4. It can be also verified analytically noting that both front and rear steering mechanisms are two four-bar mechanisms controlled by the same crank.

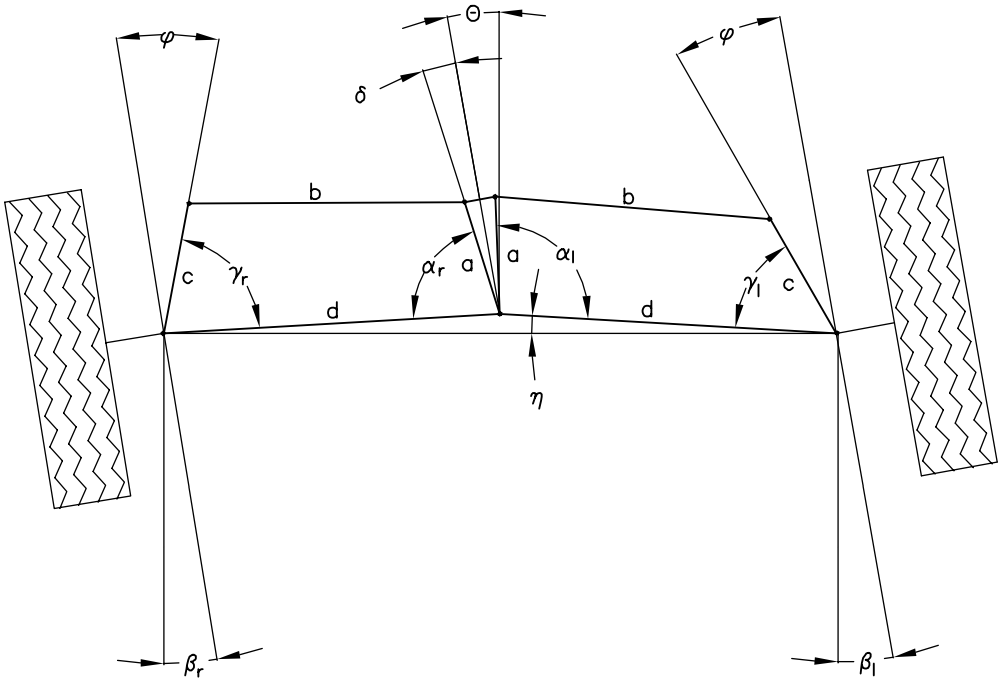

Figure 3. Front Axle Steering -- Four-bar Convention

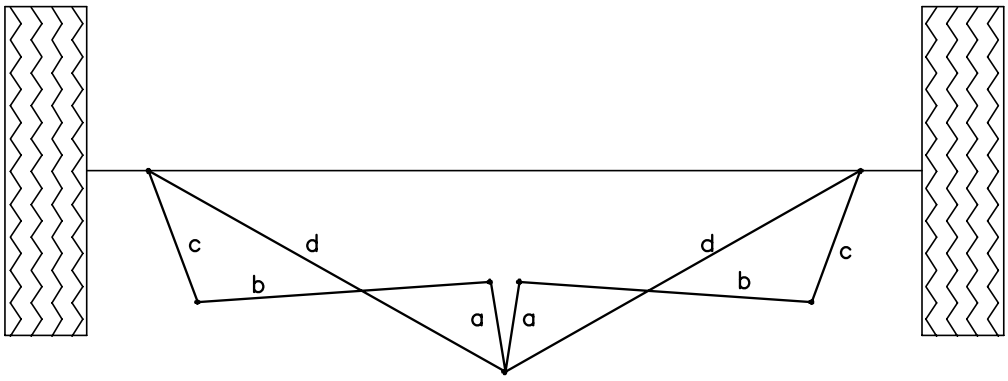

Figure 4. Rear Axle Steering -- Four-bar Convention

2.2 Suggested Design Modifications

There are several levels of modifications that can be applied to the steering mechanism in order to bring it in line with the above mentioned requirements. In order to bring the tire perpendiculars intersection to the lateral centerline the following modifications are suggested (see figure 5):

Front steering mechanism:

move the joint of the tie-rods on steering crank 30mm to the front and 15mm out.

Rear steering mechanism:

move the steering crank pivot point 40mm forward and the tie-rods joints 15mm out.

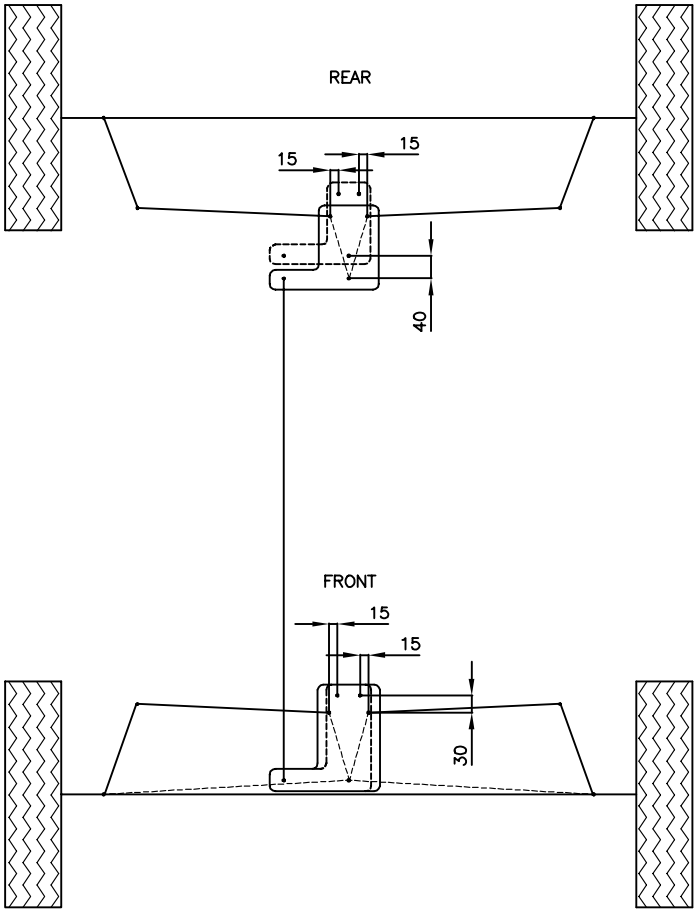

Figure 5. Steering Mechanism Proposed Changes

As figure 6 shows, this will approximately achieve the desired steering kinematics. Further calculations are suggested if more accurate results are desired. Furthermore, by moving the rear

steering crank 40mm forward, the tie-rods will interfere with the battery holder. A decision must be made whether to move the battery holder forward or move the crank less than 40mm. If the latter option is chosen, the perpendiculars from the tires will intersect forward of the lateral centerline.

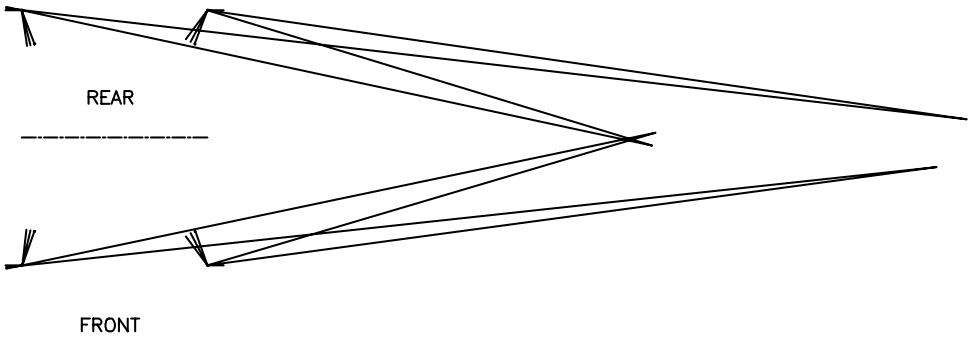

Figure 6. Steering Mechanism Proposed Changes Center of Curvature

If both perfect steering symmetry and correct steering angles need to be achieved, then figure 7 suggests a mechanism that will achieve this goal. A series of "in-between" designs can be implemented depending on the amount of modifications that is feasible. Furthermore, a vehicle model that takes into account the large amount of slip can be considered and the direction can be controlled in spite of the steering mechanism's deficiencies.

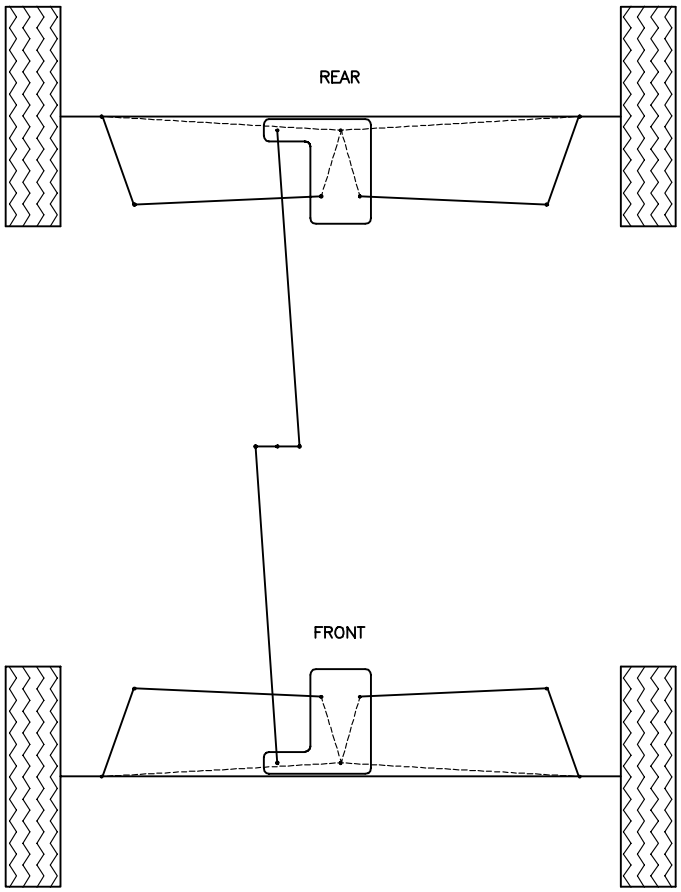

Figure 7. Steering Mechanism with Perfect Symmetry

2.3 Modeling

As mentioned in the previous section, the steering mechanism can be analyzed as a symmetric double four-bar mechanism with a shared crank. Figure 3 shows the angles and lengths conventions used in the analysis for the front steering mechanism. Figures 8 and 9 show the actual dimensions of the front and rear steering mechanisms.

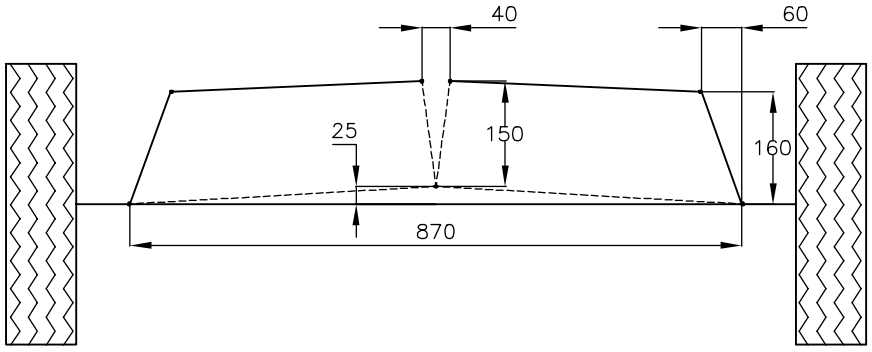

Figure 8. Front Axle Steering Dimensions

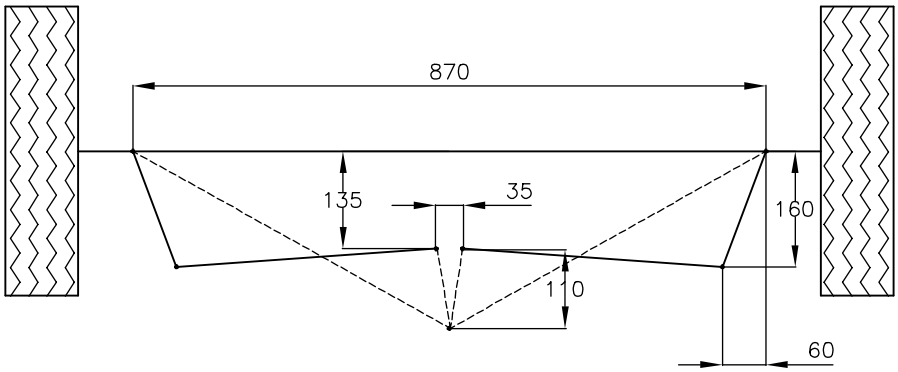

Figure 9. Rear Axle Steering Dimensions

An analysis of the four-bar mechanism yields the following static relation between the input angle, output angle and the lengths of the bars:

$$\frac{a^2 - b^2 + c^2 + d^2}{2} = cd\cos(\gamma) + ad\cos(\alpha) - ac\cos(\gamma + \alpha) \tag{1}$$

From this, a dynamic relationship can be established between the input and output angles.

$$\dot{\gamma} = \dot{\alpha}\frac{ad\sin(\alpha) - ac\sin(\gamma + \alpha)}{ac\sin(\gamma + \alpha) - cd\sin(\gamma)} \tag{2}$$

Since the four-bar input angles for the right and left sides are equal only when the crank angle (Θ) is zero, indexes must be used to differentiate the two sides. The following static relations exist between the crank angle and the four-bars input angles:

$$\alpha_r + \theta + \delta - \eta - \frac{\pi}{2} = 0 \tag{3a}$$

$$\alpha_l - \theta + \delta - \eta - \frac{\pi}{2} = 0 \tag{3b}$$

And thus the dynamic relation between these angles is

$$\dot{\alpha}_r = -\dot{\theta} \tag{4a}$$

$$\dot{\alpha}_l = \dot{\theta} \tag{4b}$$

Similarly there are static and dynamic relationships between the four-bars output angles and the steering angles.

$$\gamma_r - \beta_r + \phi + \eta - \frac{\pi}{2} = 0 \tag{5a}$$

$$\gamma_l + \beta_l + \phi + \eta - \frac{\pi}{2} = 0 \tag{5b}$$

$$\dot{\beta}_r = \dot{\gamma}_r \tag{6a}$$

$$\dot{\beta}_l = -\dot{\gamma}_l \tag{6b}$$

The steering is commanded through an electric linear actuator acting on the steering crank. The geometry of the actuator is presented in figure 10.

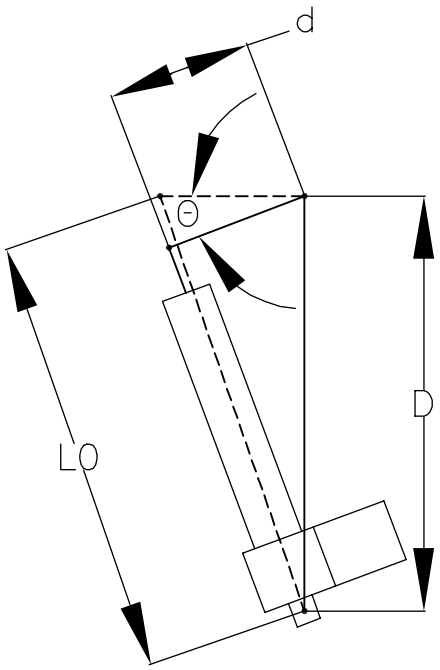

Figure 10. Steering Actuator Convention

It can be derived that the static relation between the displacement of the linear actuator and the crank angle is

$$\sin(\theta) = \frac{D^2 + d^2 - (L_0 + l)^2}{2Dd} \tag{7}$$

Therefore the dynamic relation between the steering crank angle and the linear actuator displacement is

$$\dot{\theta} = -\dot{l}\,\frac{(L_0 + l)}{Dd\cos(\theta)} \tag{8}$$

The dynamics of the motor of the linear actuator can be represented by the following dynamic equations:

$$\dot{\omega} = \frac{(K_a i - b\omega)}{J} \tag{9a}$$

$$\dot{i} = \frac{\left(v - Ri - K_a \omega\right)}{L} \tag{9b}$$

where

ω - motor speed

i - current

J - motor inertia

L - coil inductance

R - coil resistance

b - viscous friction coefficient

K_a - torque constant

v - input voltage

The relation between the motor speed and the linear actuator displacement is

$$\dot{l} = \omega ?r \tag{10}$$

Finally, using equations (2), (4a), (6a), (8) and (10), an expression between the linear actuator motor speed and the right side steering angle is obtained.

$$\dot{\beta}_r = \omega \frac{r\left(L_0 + l\right)}{Dd\cos(\theta)} \frac{ad\sin(\alpha_r) - ac\sin(\alpha_r + \gamma_r)}{ac\sin(\alpha_r + \gamma_r) - cd\sin(\gamma_r)} \tag{11}$$

Similarly, using equations (2), (4b), (6b), (8) and (10), an expression for the left side steering angle can be derived.

2.4 Steering Model Simulation

The above equations have been implemented in a simulation that has as input the voltage to the linear actuator motor and as output all the angles and lengths necessary to rebuild the steering mechanism. Figure 11 shows one example of output containing the steering crank angle and the left and right steering angles. The output can also be used in an animation that displays on screen the kinematics of the steering mechanism.

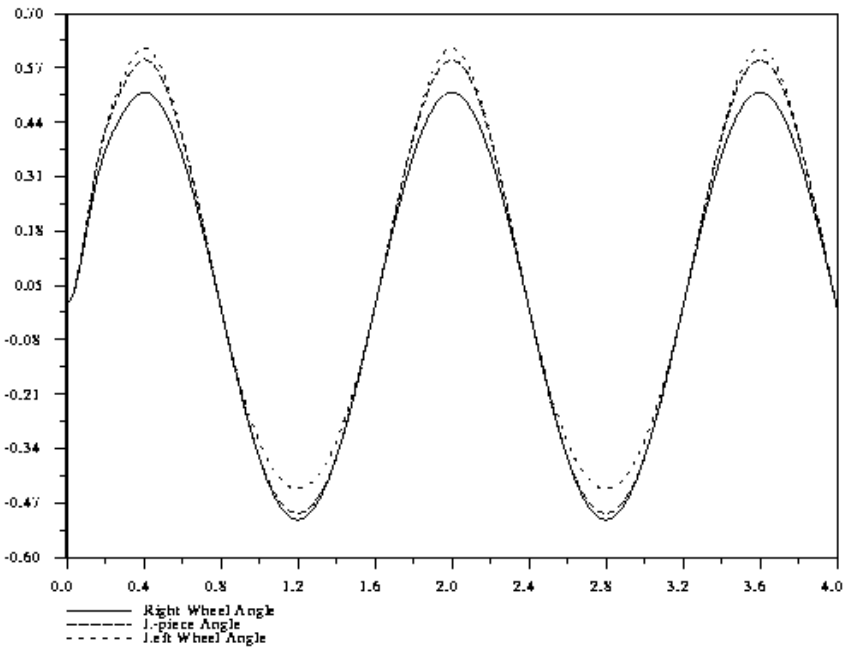

Figure 11. Steering Angles

CAUTION: Since many of the parameters needed to implement equations (9a) and (9b) are unknown, "reasonable" values have been used. Therefore the simulation and the associated animation currently present only a qualitative image and not a quantitative one.

2.5 Control

Due to the nonlinearities and model uncertainties present in the system, a Sliding Mode Controller is suggested. The desired output is taken to be one of the steering angles and the input is the voltage to the linear actuator motor. Therefore, in the normal Sliding Mode formulation, the definition of the sliding surface would be

$$S = \frac{d}{dt} + \lambda \int e \tag{12}$$

where $e = \beta - \beta_{des}$

However, such formulation involves the differentiation of equation (2) which is not only complicated but adds a large amount of uncertainty in the control formulation. Therefore a multiple surface Sliding Mode Control will be implemented. The idea is to use two sliding

surfaces with an intermediate input/output. In this case, the intermediate input/output will be taken to be ω. The first surface is then defined as

$$S_1 = \beta - \beta_{des} \tag{13}$$

which, when differentiated once yields

$$\dot{S}_1 = \dot{\beta} - \dot{\beta}_{des} \tag{14}$$

Inserting equation (11) in (14) yields

$$\dot{S}_1 = \omega \frac{r\left(L_0 + l\right)}{Dd\cos(\theta)} \frac{ad\sin(\alpha_r) - ac\sin(\alpha_r + \gamma_r)}{ac\sin(\alpha_r + \gamma_r) - cd\sin(\gamma_r)} - \dot{\beta}_{r\_des} \tag{15}$$

In order to achieve the "smooth" sliding condition

$$\dot{S} = -kS \tag{16}$$

ω must be such that

$$\omega_{des} = \frac{Dd\cos(\theta)}{r\left(L_0 + l\right)} \frac{ac\sin(\alpha_r + \gamma_r) - cd\sin(\gamma_r)}{ad\sin(\alpha_r) - ac\sin(\alpha_r + \gamma_r)} \left(\dot{\beta}_{r\_des} - k_1 S_1\right) \tag{17}$$

where k_1 includes the model uncertainties.

Using the above formulation, the second error is defined as

$$e_2 = \omega - \omega_{des} \tag{18}$$

and the second sliding surface

$$S_2 = e_2 + \lambda e_2 \tag{19}$$

Differentiating equation (19) once yields

$$\dot{S}_2 = \dot{e}_2 + \lambda \dot{e}_2 = \ddot{\omega} - \ddot{\omega}_{des} + \lambda \dot{e}_2 \tag{20}$$

Differentiating equation (9a) and substituting in equation (20) the following definition of $\dot{S}_2$ is obtained:

$$\begin{aligned} \dot{S}_2 &= \frac{K_a}{J}\dot{i} - \frac{b}{J}\dot{\omega} - \ddot{\omega}_{des} + \lambda \dot{e}_2 \\ &= \frac{K_a}{JL}\left(v - Ri - K_a\omega\right) - \frac{b}{J^2}\left(K_a i - b\omega\right) - \ddot{\omega}_{des} + \lambda \dot{e}_2 \end{aligned} \tag{21}$$

As before, equation 16 must be satisfied so v must be

$$v = \frac{JL}{K_a}\left[\frac{K_a}{JL}\left(Ri + K_a\omega\right) + \frac{b}{J^2}\left(K_a i - b\omega\right) + \ddot{\omega}_{des} - \lambda \dot{e}_2 - k_2 S_2\right] \tag{22}$$

Where again k_2 contains the model uncertainties.

2.6 Simulation

The above equations were implemented in simulation. Figure 12 shows the actual and desired right steering angle, while figure 13 shows these two angles together with the steering crank angle and the left steering angle.

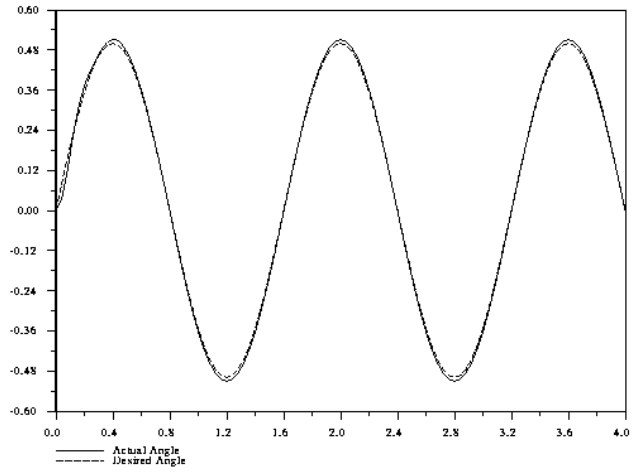

Figure 12. Actual and Desired Right Steering Angle

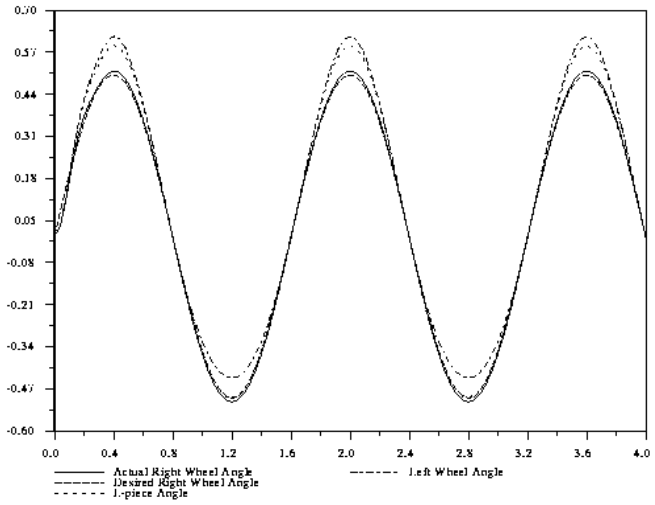

Figure 13. Actual and Desired Right Steering, Steering Crank and Left Steering Angles

3. Brakes

3.1 Description

The vehicle is equipped with a motor at each wheel which will also provide the braking under normal driving situations. However, for the case when additional braking is required, the vehicle is also equipped with a set of four independent electro-mechanically actuated drum brakes. The following sections will attempt to provide a model of the brake actuation, a control algorithm and a model of the drum brakes.

3.2 Actuation Model

The drum brakes are actuated through an electric motor which pulls on a cable attached to a spring which in turn applies the brakes. The model of the actuator is that of an electric motor with the addition of the torque opposed by the spring. A schematic of the actuator can be seen in figure 14.

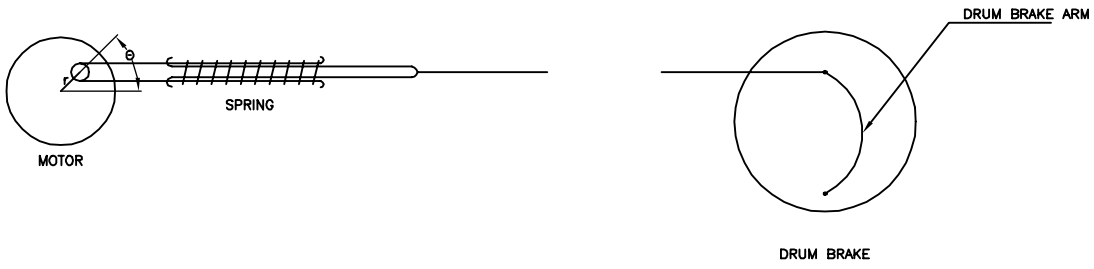

Figure 14. Brake Actuation Diagram and Convention

The following equations can be written:

$$\dot{\theta} = \omega \tag{23a}$$

$$\dot{\omega} = \frac{\left(K_a i - b\omega - Fr\sin(\theta)\right)}{J} \tag{23b}$$

$$\dot{i} = \frac{\left(v - Ri - K_a \omega\right)}{L} \tag{23c}$$

$$\dot{F} = K_s \sin(\theta)\omega r \tag{23d}$$

where

θ - motor angle

ω - motor speed

i - current

F - spring (brake actuation) force

K_a - torque constant

b - viscous friction coefficient

R - coil resistance

L - coil inductance

J - motor inertia

K_S - spring constant

r - motor arm length

F can also be written statically as a function of θ as $F = K_s(1-\cos\theta)r$. From this, θ =θ (F) can be derived.

3.3 Control

Again, a Sliding Mode Control formulation was implemented. The output is the motor angle θ which is related to the actuation force as above and the input is the voltage. The error is thus defined as

$$e = \theta - \theta_{des} \tag{24}$$

and the sliding surface as

$$S = \dot{e} + 2\lambda e + \lambda^2 e \tag{25}$$

Differentiating once yields

$$\dot{S} = \ddot{e} + 2\lambda \dot{e} + \lambda^2 \dot{e} \tag{26}$$

Using equations (23) and substituting in (26) the following expression is obtained:

$$\dot{S} = \frac{K_a}{JL} v - \frac{R}{L} i - \frac{K_a}{L} \omega - \frac{b}{J} \dot{\omega} - \frac{K_s r^2}{J} \omega \left(\cos\theta - \sin^2\theta + \cos^2\theta \right) - \ddot{\theta}_{des} + 2\lambda \ddot{e} + \lambda^2 \dot{e} \tag{27}$$

Therefore the input voltage must be

$$v = \frac{JL}{K_a} \left(\frac{K_a}{J} \frac{R}{L} i + \frac{K_a}{L} \omega + \frac{b}{J} \dot{\omega} + \frac{K_s r^2}{J} \omega \left(\cos\theta - \sin^2\theta + \cos^2\theta \right) + \dddot{\theta}_{des} - 2\lambda \ddot{e} - \lambda^2 \dot{e} - kS \right) \tag{28}$$

3.4 Simulation

As in the case of the steering a simulation program was developed. Figure 15 shows the actual and desired motor angle for a sinusoidal case. Figure 16 shows the equivalent actual and desired actuation force, while figure 17 presents the voltage input required for this maneuver. Figures 18 and 19 show the desired and actual motor angle and actuation force in the case of a first order response desired output. The dynamics of the response of the actual force can be changed by changing the dynamics of S.

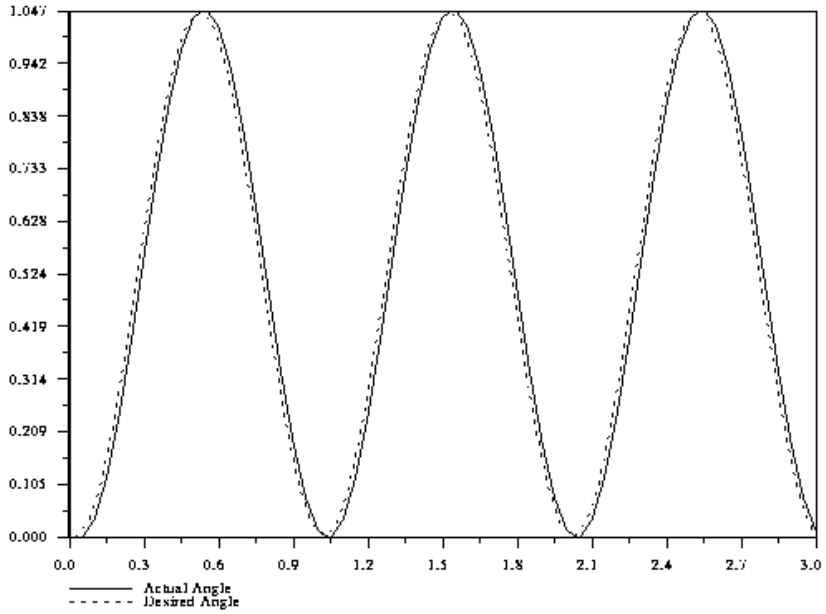

Figure 15. Actual and Desired Motor Angle for a Sinusoidal Case

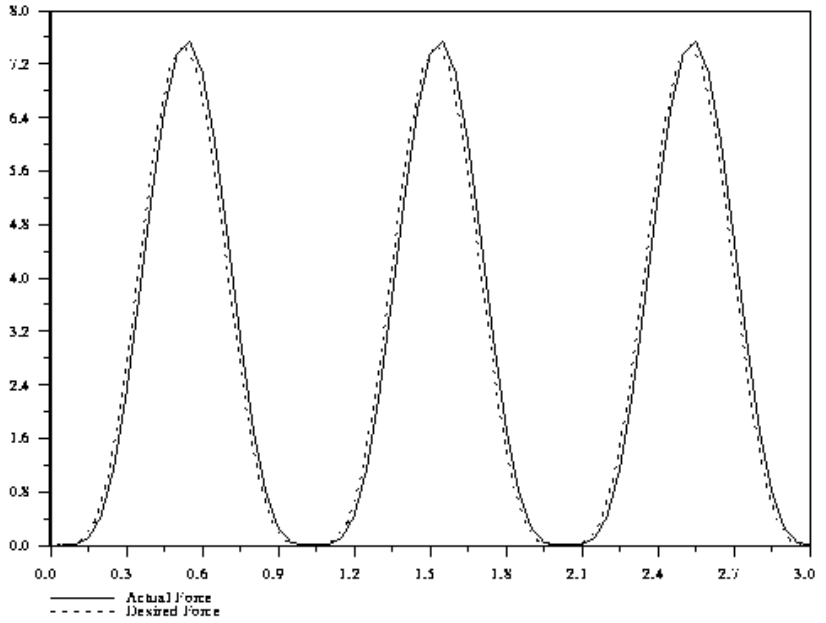

Figure 16. Actual and Desired Actuation Force

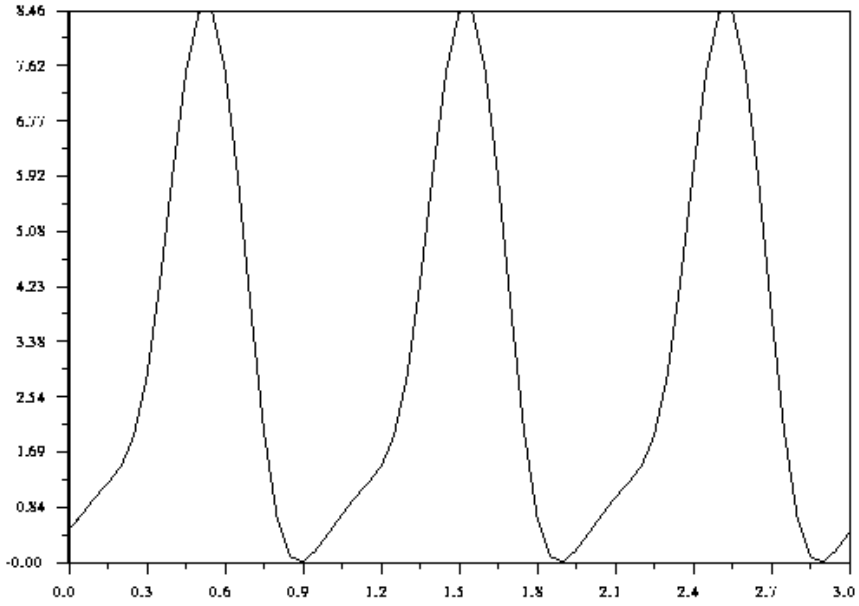

Figure 17. Brake Voltage Input

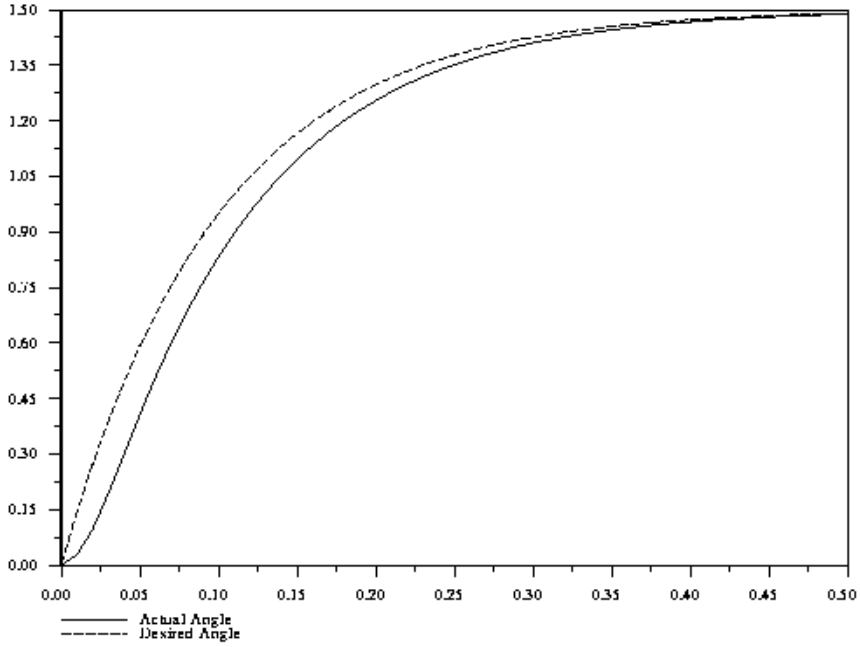

Figure 18. Actual and Desired Brake Actuator Motor Angle -- First Order Desired Response

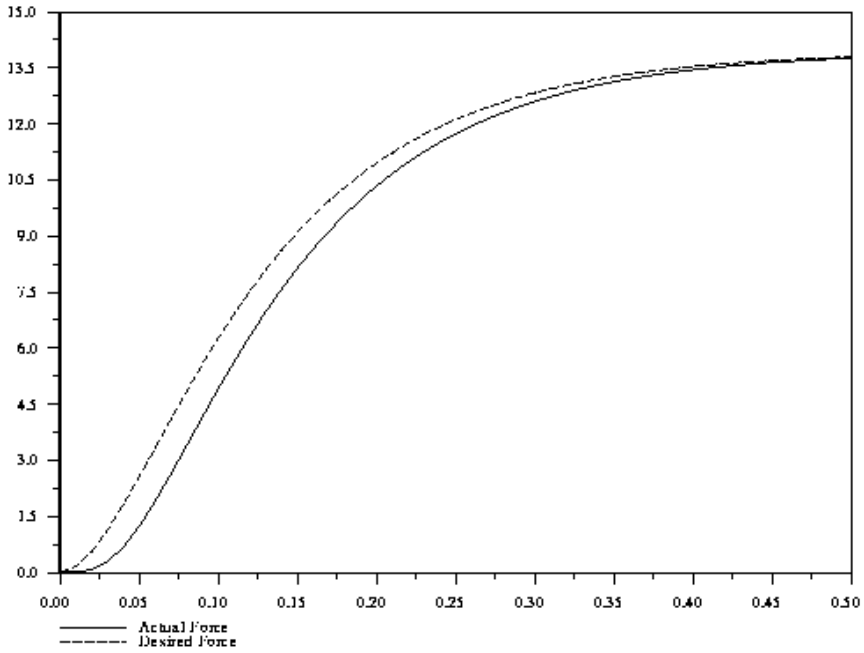

Figure 19. Actual and Desired Brake Actuator Motor Force -- First Order Desired Response

As before, the simulation was run with "reasonable" values. Some, as in the case of the spring constant, may be good guesses. The value used in simulation was 1000 N/m while the measured value turned out to be 1255 N/m. Other parameters, which have not been measured yet, may not be that accurate.

3.5 Drum Brakes Model

Once a desired brake actuation force is obtained, the equivalent brake torque needs to be obtained. This section will present a model of the drum brakes. Figure 20 shows the relevant dimensions of the drum brakes while figure 21 details the operation. As it can be seen from figure 21, when the force acts on the brake drum arm it creates a torque in the brake drum actuator that pushes the two brake shoes apart and against the rotating drum. It is important to note that the displacement of the brake shoes is *minimal.* When the pads are new they actually drag on the drum even when the brakes are not applied. As they wear out, since these particular brakes are not self-adjusting, there will be a small amount of travel.

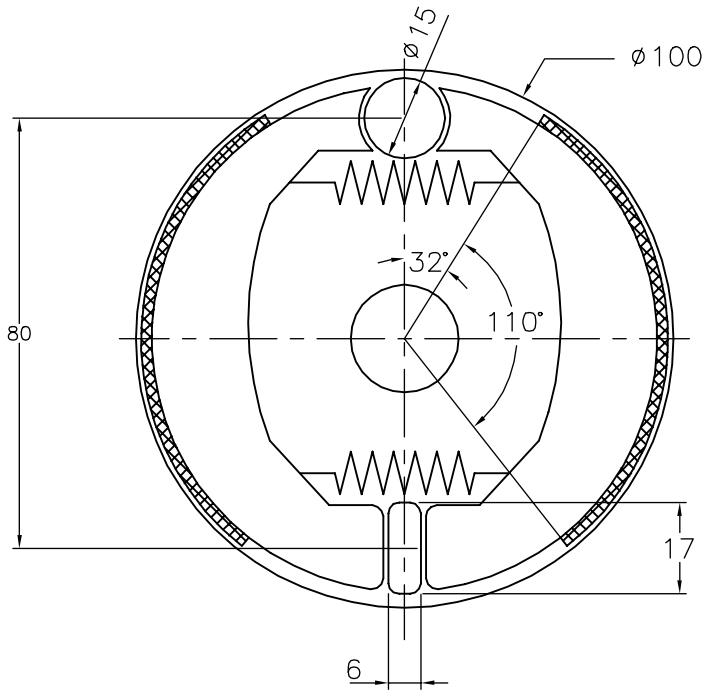

Figure 20. Brake Drum Dimensions

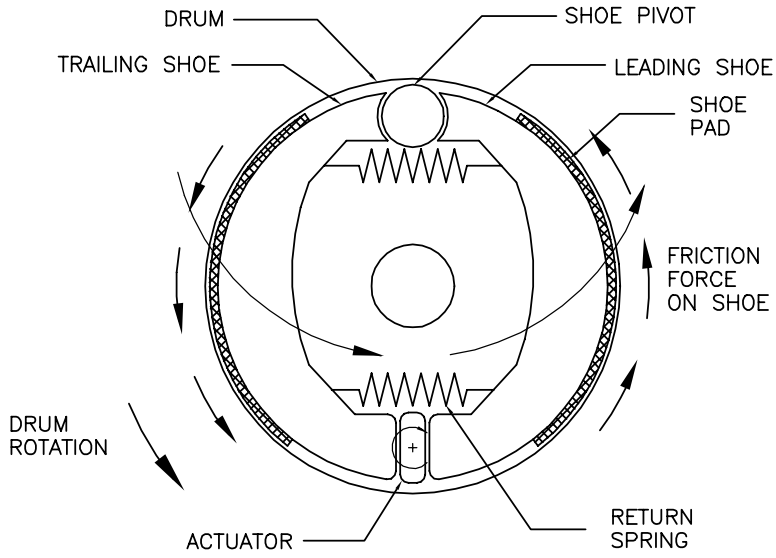

Figure 21. Brake Drum Functionality

Second important thing to notice from figure 21 is that these brakes are "single leading" or "leading/trailing" type. As it can be seen from the orientation of the friction force on the shoes, the leading shoe will be attracted towards the drum providing even more friction force while the trailing shoe will be pushed away from the drum, providing less friction force. Whether a shoe is

leading or trailing depends on the direction of the rotation of the drum. Thus a leading shoe in forward motion of the vehicle becomes a trailing shoe in reverse operation.

Finally, no braking force will be obtained until the preload on the return spring is overcome.

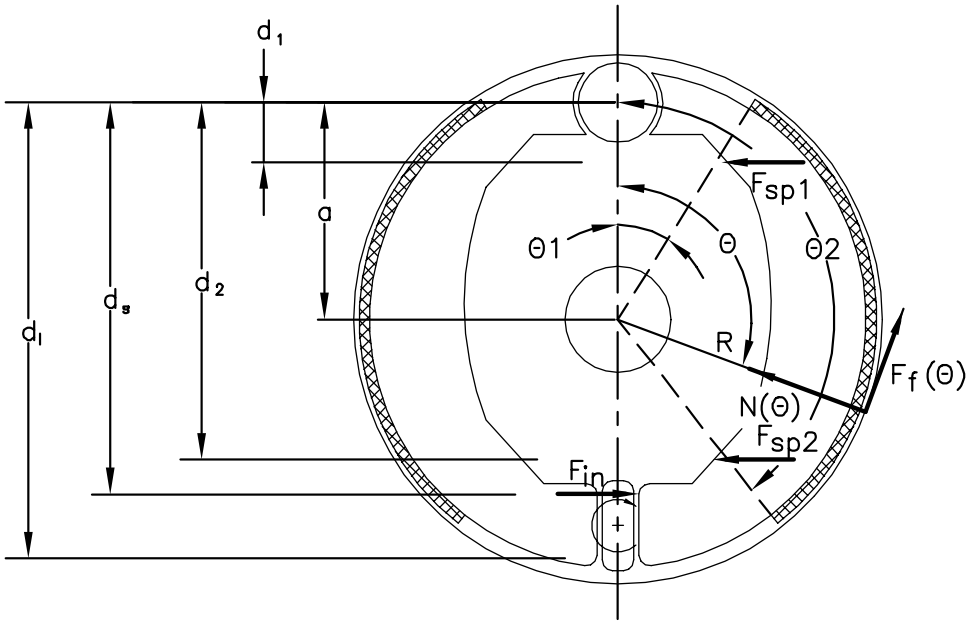

Figure 22. Drum Brake Angle and Force Convention.

From figure 22 it can be seen that at any angle θ from the pivot there acts a differential normal force dN :

$$dN = bp(\theta)Rd\theta \tag{29}$$

where b is the face width of the shoe.

The frictional forces have a moment a moment arm about the pin of $R - a\cos\theta$. The moment of the frictional forces is:

$$M_f = \mu dN(R - a\cos\theta) = \int_{\theta_1}^{\theta_2} \mu bp(\theta)R(R - a\cos\theta)d\theta \tag{30}$$

The moment arm for the normal forces is $a\sin\theta$. The moment of the normal forces is:

$$M_N = dN(a\sin\theta) = \int_{\theta_2}^{\theta_1} bp(\theta)Ra\sin\theta d\theta \tag{31}$$

Referring to figure 22, the moment balance on the leading shoe yields

$$F_{in}d_s - F_{sp1}d_1 - F_{sp2}d_2 + M_f - M_N = 0 \tag{32a}$$

and on the trailing shoe

$$F_{in}d_l - F_{sp1}d_1 - F_{sp2}d_2 - M_f - M_N = 0 \tag{32b}$$

Note that the normal force on the trailing shoe is not the same as the one on the leading shoe.

The brake torque obtained from *one* of the shoes is

$$T = \int \mu R dN = \int_{\theta_1}^{\theta_2} \mu bp(\theta)R^2 d\theta \tag{32}$$

The total brake torque is the sum of the torques generated by the two shoes.

The problem can be further simplified if a certain pressure distribution is assumed. A reasonable one is

$$p(\theta) = p_a \frac{\sin\theta}{\sin\theta_a} \tag{33}$$

where p_a is the maximum pressure located at the angle θ_a . It can be seen that θ_a occurs at 90°, or if θ_2 is less than 90°, then the maximum will occur at θ_2 . In this case one only needs to solve for p_a , a trivial task.

It is important to note that μ can vary with temperature, speed, friction material, etc.

4. Suggested Future Work

4.1 Brake Actuation Model and Simulation

When the brake actuation model was developed it was assumed that there is a direct drive from the motor to the arm. In such a case, as the model shows, a *reduction* in the input voltage would result in a reduction in the applied force. However, since the motor is equipped with a gear box and an infinite screw, a *negative* voltage must be applied in order to reduce the angle (force). The pitch of the infinite screw must be known in order to determine the torque components. Some details can be found in figure 23.

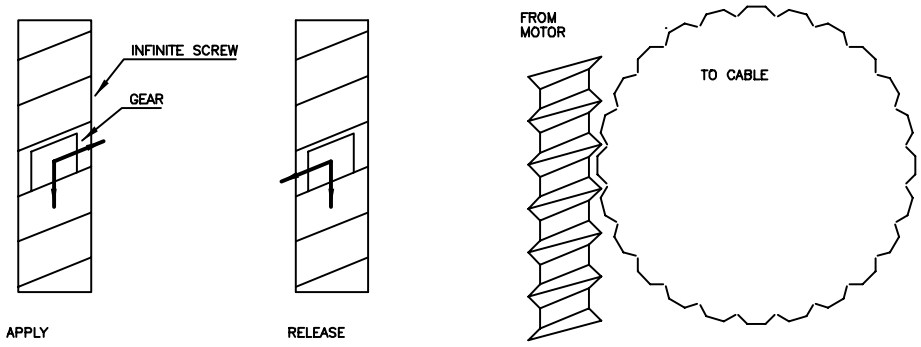

Figure 23. Brake Motor Gear Box -- Force Diagram and Schematic

Furthermore, r and J must be calculate to reflect the gearbox ratio. Simulations need to be performed in order to validate this model.

4.2 Brake Torque Model

The brake torque model should be implemented in a simulation for the whole vehicle to analyze both deceleration and the effect of distributed braking on stability and control.

4.3 Vehicle Model Simulation

In order to obtain the desired steering angles and brake torques, a lateral/longitudinal vehicle model needs to be implemented in simulation. The one suggested by Tomizuka and Pham could be used.